

# Monitoring Reaction Kinetics in Solution by Continuous-Flow Methods: The Effects of Convection and Molecular Diffusion under Laminar Flow Conditions

Lars Konermann\*

Department of Chemistry, The University of Western Ontario, London, ON, N6A 5B7, Canada

Received: March 9, 1999; In Final Form: July 7, 1999

Continuous-flow methods are a simple and efficient tool for monitoring the kinetics of chemical reactions in solution. After a reaction has been initiated by a mixing step, liquid flows down an observation tube while the reaction proceeds. The kinetics can be monitored by suitable detectors that are positioned downstream from the mixing point, assuming that the distance from the mixer is linearly related to the “age” of the reaction mixture. It is widely accepted that kinetic experiments of this kind necessarily require turbulent flow in the observation tube, which implies considerable sample consumption due to high flow velocities and large tube diameters. Reduction of flow velocity and tube diameter leads to laminar flow which is characterized by a maximum velocity in the center of the tube and a zero velocity at the tube walls, therefore resulting in a “blurring” of the time axis. However, a number of recent continuous-flow studies that were carried out under these conditions (Konermann et al. *Biochemistry* 1997, 36, 5554–5559. Konermann et al. *Biochemistry* 1997, 36, 6448–6454. Zechel et al. *Biochemistry* 1998, 37, 7664–7669) have indicated that the extent of the dispersion problem is much less pronounced than might be anticipated. In this work, detailed computer simulations are used to study the effects of laminar flow on continuous-flow experiments. It is shown that the distortion of the measured kinetics under laminar flow conditions is surprisingly small, especially when the reaction occurs on a time scale where molecular diffusion in the tube has notable effects on the age distribution function. The results of this study clearly indicate the feasibility of continuous-flow experiments in the laminar flow regime.

## Introduction

Extensive knowledge regarding the mechanisms of protein folding, enzymatic and biological electron transfer reactions comes from kinetic experiments in the time range of milliseconds to some tens of seconds. These experiments allow the detection and structural characterization of transient reaction intermediates as well as the measurement of rate constants and activation energies. The kinetics of reactions in solution may be monitored in two different ways. In the stopped-flow method, two or more reactants are rapidly mixed and then transferred to an observation cell where the kinetics can be monitored by optical spectroscopy.<sup>1–4</sup> The stopped-flow technique is often used in conjunction with chemical quenching which allows off-line analysis of reaction intermediates by NMR, mass spectrometry (MS), or other methods.<sup>5,6</sup>

In the historically older continuous-flow method, the reactants are mixed and the reaction occurs while the mixture flows down an observation tube. The age of the reaction mixture (i.e., the reaction time) depends on the distance between the mixing and observation points. It is a simple matter to monitor the reaction kinetics downstream from the mixing point by suitable detectors at different positions along the tube.<sup>4,7–11</sup> By using CCD arrays, a very large number of points along the tube can be monitored simultaneously, which greatly simplifies the experiment.<sup>12,13</sup> One important advantage of the continuous-flow method is that detectors with long response times can be used since the kinetics are not monitored in real time. Another advantage is that the time resolution in these experiments can be on the order of 50

$\mu\text{s}$ , which is a factor of 30 better than the resolution obtainable in stopped-flow devices.<sup>12</sup> A similar time resolution can be obtained in pulsed/continuous-flow experiments by using integrating observation.<sup>14,15</sup> This modified technique requires somewhat smaller reactant volumes than traditional continuous-flow experiments. However, the sample consumption is still significantly higher than in stopped-flow experiments.

Turbulent flow in the observation tube is widely regarded as an absolutely essential requirement for kinetic continuous-flow experiments in solution.<sup>1,2,7,8,14</sup> Turbulent flow leads to continuous mixing of fast and slow liquid in the tube. Data analysis under these conditions is commonly carried out as if the flow velocity were constant across the tube (“homogeneous” flow). Turbulent flow in a tube can be predicted by calculating the Reynolds number  $\mathcal{R}$

$$\mathcal{R} = \frac{\bar{v}d\rho}{\eta} \quad (1)$$

where  $\bar{v}$  is the average flow velocity,  $d$  is the tube diameter,  $\rho$  is the density, and  $\eta$  is the viscosity. Turbulent flow occurs when  $\mathcal{R}$  exceeds 2000.<sup>2,16</sup>

For  $\mathcal{R} < 2000$ , the flow is laminar and has a parabolic velocity profile. Under these conditions, the velocity  $v$  as a function of radial position  $r$  for a circular tube with radius  $R$  is given by<sup>17</sup>

$$v(r) = v_{\max} \left( 1 - \frac{r^2}{R^2} \right) \quad (2)$$

The flow velocity at the center of the tube,  $v_{\max}$ , is twice the average flow velocity  $\bar{v}$ . The dispersion of reactants and products

\* To whom correspondence should be addressed. E-mail: konerman@julian.uwo.ca. Phone: (519) 679-2111 ext. 6313. FAX: (519) 661-3022. Internet: <http://www.uwo.ca/chem/faculty/konermann.html>.

caused by the variation in the flow velocity across the tube will blur the time axis, which could lead to a substantial distortion of the observed kinetics. In fact, it appears that meaningful kinetic experiments under laminar flow conditions might be impossible.

However, this does not seem to be the case. In a number of recent studies, a continuous-flow setup was coupled to an electrospray ionization mass spectrometer for monitoring the kinetics of protein folding<sup>18,19</sup> and enzymatic reactions.<sup>20</sup> The flow tube in these experiments had a diameter of only 75  $\mu\text{m}$  and flow rates were as low as 10 to 30  $\mu\text{L}/\text{min}$ , resulting in a Reynolds number between 2.8 and 8.5, which implies laminar flow. Surprisingly, it was found that the kinetics monitored by this device agreed very well with results obtained by conventional stopped-flow methods. This raises the question whether turbulent flow is required for these experiments or not. Answering this question is important for kineticists since continuous-flow instruments operating under laminar flow conditions could be very useful because of their versatility, low cost, and low sample consumption. Up to now, the effects of laminar flow on kinetic experiments in solution have not been studied in detail. Earlier work<sup>9</sup> has treated this question only superficially, leaving open questions regarding the nature of the processes occurring in the observation tube and at the detector. Interestingly, continuous-flow measurements under laminar flow conditions have been used for many years to study the kinetics of chemical reactions in the gas phase with high precision.<sup>21,22</sup> None of these gas-phase flow techniques rely on specific properties of the carrying medium. Therefore, it appears that meaningful kinetic measurements under laminar flow conditions should be possible not only for gas-phase reactions.

The goal of the present study is to clarify the effects of laminar flow on kinetic continuous-flow experiments in solution. Computer simulations of kinetics measured under laminar flow conditions are compared to data that would be observed in a hypothetical ideal continuous-flow setup with homogeneous flow. It is shown that laminar flow can somewhat distort the observed kinetics, but the magnitude of these effects appears to be modest. Diffusion of analyte molecules in the tube can almost eliminate these distortions so that the observed kinetics are often virtually identical to those that would be observed under homogeneous flow conditions. To allow a direct comparison to recent experimental work,<sup>18–20,23</sup> the calculations in this study were carried out for an observation tube with an inner diameter of 75  $\mu\text{m}$  and an average flow velocity  $\bar{v}$  of 0.113 m/s, which corresponds to a flow rate of 30  $\mu\text{L}/\text{min}$ .

## Theory

For continuous-flow experiments, it is necessary to distinguish two types of detectors. A “type I detector” monitors the cross-sectional area of the tube at a certain longitudinal position and counts the number of analyte molecules that flow through this plane per time unit. An example of such a detector is an electrospray ionization mass spectrometer that monitors molecules at the exit of a capillary.<sup>24</sup> A “type II detector” monitors the average concentration in the tube at a certain longitudinal position. Examples of type II detectors are optical devices such as spectrophotometers or fluorimeters.

Consider a large number of analyte molecules that flow through an observation tube oriented along the  $x$ -axis of a cylindrical coordinate system. Molecules enter the tube at  $x = 0$ . The age  $a$  of a molecule at a longitudinal position  $x = l$  is defined as the time that has elapsed since the molecule has passed  $x = 0$ . The variable  $\tau = l/\bar{v}$  (in units of seconds) is used

to establish a time axis along the observation tube. If  $P(a)$  is the probability that an analyte molecule at  $x = l$  has an age in the range  $a$  to  $a + da$  then the average age  $\langle a \rangle$  of the analyte at  $x = l$  is given by

$$\langle a \rangle = \int_0^{\infty} aP(a) da \quad (3)$$

In the hypothetical case of homogeneous flow [ $v(r) = \bar{v}$ ],  $P(a)$  is given by a Dirac function  $P(a) = \delta(a - \tau)$  and

$$\langle a \rangle = \int_0^{\infty} a \delta(a - \tau) da = \tau \quad (4)$$

Now consider a chemical reaction where, in an isolated reaction vessel (i.e., not a flow device), the time-dependent concentration of a molecular species would be given by  $C(t)$ . For studying the kinetics of this reaction in a continuous-flow experiment, it is assumed that reactant mixing at  $x = 0$  occurs instantaneously and that the dimensions of the mixer are small compared to the volume of the observation tube. A type I or type II detector located at  $x = l$  will measure an average concentration  $\langle C \rangle$  that is given by

$$\langle C \rangle = \int_0^{\infty} C(a) P(a) da \quad (5)$$

The analysis of kinetic continuous-flow experiments is usually carried out as if the flow in the tube were homogeneous. In these cases, it is assumed that

$$\langle C \rangle \approx \int_0^{\infty} C(a) \delta(a - \tau) da = C(\tau) \quad (6)$$

Under laminar flow conditions, this approximation is not appropriate. Instead, the characteristics of the age distribution function  $P(a)$  have to be taken into account explicitly. We will now calculate  $P(a)$  for the limiting case where diffusion of analyte molecules in the tube can be neglected. The two types of detectors have to be considered separately.

**Age Distribution Function for a Type I Detector under Laminar Flow Conditions.** For a type I detector, molecules that travel close to the center of the tube have a stronger contribution to the overall signal than molecules that travel close to the capillary wall. This is because molecules flowing near the center line are faster, and therefore more of them cross the detector plane per time unit. For calculating  $P(a)$ , the observation tube is divided into a large number of concentric, circular layers, each of them having a wall thickness of  $dr$ . The total liquid volume  $V$  that passes through the detector plane in a time of  $T$  seconds is given by

$$V = T \int_0^R 2\pi r v(r) dr = \frac{1}{2} \pi R^2 v_{\text{max}} T \quad (7)$$

At the detector, each concentric layer of solution between  $r$  and  $r + dr$  contains molecules of age  $a = l/v(r)$ . Its contribution to the volume  $V$  is  $dV = 2\pi r v(r) T dr$ . Therefore,

$$P(a) da = \frac{dV}{V} = 4 \left( \frac{r}{R^2} - \frac{r^3}{R^4} \right) dr \quad (8)$$

With  $a = l/v(r)$  and eq 2, we obtain

$$\frac{dr}{da} = \frac{1}{2\sqrt{1 - l/(v_{\text{max}} a)}} \frac{1}{a^2} \quad (9)$$

so that  $P(a)$  is given by

$$P(a) = \frac{2l^2}{v_{\max}^2} \frac{1}{a^3} \quad \text{for } a \geq l/v_{\max}$$

and

$$P(a) = 0 \quad \text{for } a < l/v_{\max} \quad (10)$$

The average age of the solution at  $x = l$ , calculated from eq 3, is  $\langle a \rangle = l/\bar{v} = \tau$ .

**Age Distribution Function for a Type II Detector under Laminar Flow Conditions.** It follows that for a type II detector

$$P(a) da = \frac{dA}{A} = \frac{2r}{R^2} dr \quad (11)$$

where  $A = \pi R^2$  is the cross section of the tube and  $dA = 2\pi r dr$  is the area of a ring which has a width of  $dr$  and corresponds to an age  $a$ . With eqs 2 and 9,  $P(a)$  for a type II detector is

$$P(a) = \frac{l}{v_{\max}} \frac{1}{a^2} \quad \text{for } a \geq l/v_{\max}$$

and

$$P(a) = 0 \quad \text{for } a < l/v_{\max} \quad (12)$$

Plots of the age distribution functions calculated from eqs 10 and 12 are shown in Figure 1.

**Effects of Molecular Diffusion.** The age distribution functions calculated above are valid for analyte molecules that are transported through the capillary by convection only. A realistic description must take into account molecular diffusion which continuously changes the radial position and hence alters the longitudinal velocity  $v(r)$  of each molecule as it flows through the tube. Previous work<sup>25</sup> has shown that for the type of simulations carried out in this study the diffusion in the  $x$ -direction can be neglected since longitudinal movement is completely dominated by convection. Consequently, it is a good approximation to describe molecular diffusion as a two-dimensional random walk perpendicular to the tube axis. Under these conditions, the probability density  $W(s,t)$  for finding a molecule at a distance  $s$  from its original location after time  $t$  is given by<sup>26,27</sup>

$$W(s,t) = \frac{1}{4\pi Dt} e^{-s^2/(4Dt)} \quad (13)$$

From this equation, the mean square displacement  $\langle s^2 \rangle$  after time  $t$  can be calculated,

$$\langle s^2 \rangle = \int_{s=0}^{\infty} \int_{\varphi=0}^{2\pi} s^2 \frac{1}{4\pi Dt} e^{-s^2/(4Dt)} s ds d\varphi = 4Dt \quad (14)$$

### Computer Simulations

**The Model.** Deriving the age distribution function from analytical solutions of the convective-diffusion equation<sup>25,28–34</sup> is not straightforward, except for the trivial case where  $D = 0$ . In the present study,  $P(a)$  is calculated by a computer-based numerical method. In this method, the flow of analyte molecules through the combined effects of convection and diffusion is simulated by an iterative algorithm. For computing  $P(a)$ , it is assumed that these molecules are “stable”, i.e., they do not undergo a chemical reaction. Every iteration step corresponds to a time interval  $\Delta t$  ( $\Delta t$  is in the range 1–5 ms), and it consists of two parts: (i) each molecule is advanced in the  $x$ -direction according to  $\Delta x = v(r)\Delta t$ , where  $v(r)$  is given by eq 2; (ii) in

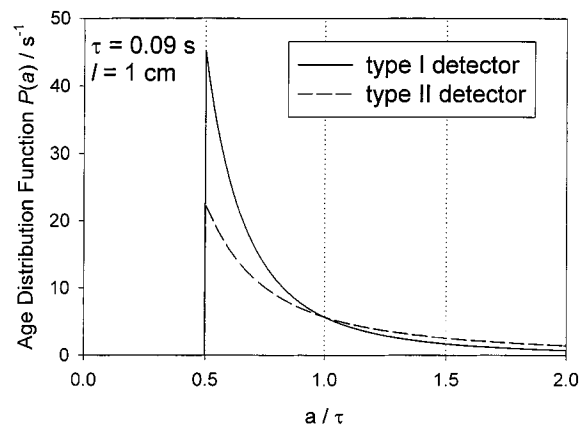


**Figure 1.** Age distribution functions for two types of detectors positioned at  $l = 1$  cm. The average flow velocity  $\bar{v}$  in this case is 0.113 m/s so that  $\tau = 0.09$  s.

the absence of convection, each molecule is displaced as the result of two-dimensional diffusion. It is assumed that  $\Delta s = 2\sqrt{D\Delta t}$  (see eq 14) so that

$$r_{\text{new}} = (r_{\text{old}}^2 + \Delta s^2 - 2r_{\text{old}}\Delta s \cos \varphi)^{1/2} \quad (15)$$

The direction  $\varphi$  of each diffusive step is taken at random from  $0 < \varphi \leq 2\pi$ . If  $r_{\text{new}}$  exceeds the radius  $R$ , the molecule is reflected from the wall and the new radial distance  $r_{\text{new}}$  becomes  $r_{\text{new}}' = 2R - r_{\text{new}}$ . The particle flow is monitored at various positions  $x = l$  by type I and type II detectors. The type II detectors monitor the average concentration in a volume of  $\pi R^2 \times 4R$ .

### Calculation of Age Distribution Functions from the Model.

Computation of the age distribution function is done by simulating the flow of a “semi-indefinite slug” of analyte molecules through the tube by the iterative process described in the last paragraph. For  $t = 0$ , the distribution of molecules in the tube is characterized by  $C(x,r,t) = 1$  for  $x < 0$  and  $C(x,r,t) = 0$  for  $x \geq 0$ . The age of each molecule, i.e., the time elapsed since it has passed  $x = 0$ , is monitored during the simulation. When a particle is detected at  $x = l$ , its age is stored in the computer memory. The age distribution function  $P(a)$  is calculated by generating a normalized histogram from the age values of a large number (typically about  $5 \times 10^5$ ) of molecules. Only those molecules are taken into account that are detected after the signal intensity has reached a constant level. A typical example for a type I detector positioned at  $l = 7.5$  cm is depicted in Figure 2.

### Results

**Validity of the Model.** The computer model described above provides a simple approximate description for the effects of convection and diffusion on analyte molecules that flow through a circular tube under laminar flow conditions. Before this model is used for calculating age distribution functions under different conditions, its validity has to be tested. Figure 3 shows results of simulations for the flow of a thin sample plug through a tube. The average concentration monitored by a type II detector at different positions  $x = l$  is plotted as a function of time. Initially ( $t = 0$ ), all the molecules are distributed uniformly across the cross section of the tube at  $x = 0$ . Curve 1 shows the result of a simulation for  $l = 32$  cm in the absence of molecular diffusion. The dispersion of the analyte is clearly evident. The leading edge of the signal is detected at  $t = l/(2\bar{v})$ . Its tailing portion is due to slowly flowing molecules at successively larger radial

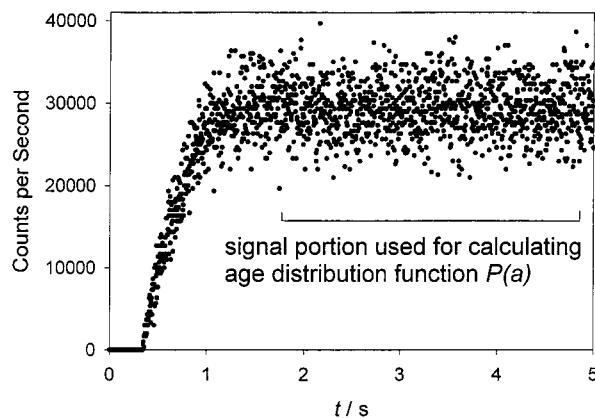


**Figure 2.** Signal monitored by a type II detector for a “semi-infinite slug” of analyte molecules that flows through an observation tube. The portion of the signal that is used for extracting the age distribution function  $P(a)$  is indicated. Parameters used in this simulation:  $D = 5 \times 10^{-10} \text{ m}^2/\text{s}$ ;  $d = 75 \text{ }\mu\text{m}$ ;  $\bar{v} = 0.113 \text{ m/s}$ .

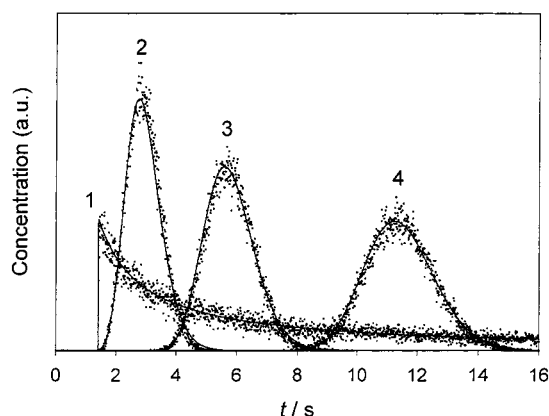


**Figure 3.** Flow of a thin sample plug through an observation tube. Shown is the average concentration (monitored by a type II detector) in the tube as a function of time at different positions  $l$ . Scattered points are obtained from current simulations, solid lines are theoretical curves taken from the literature (see text). Data are shown for the following conditions: (1)  $D = 0 \text{ m}^2/\text{s}$ ,  $l = 32 \text{ cm}$ ; (2)  $D = 5 \times 10^{-10} \text{ m}^2/\text{s}$ ,  $l = 32 \text{ cm}$ ; (3)  $D = 5 \times 10^{-10} \text{ m}^2/\text{s}$ ,  $l = 64 \text{ cm}$ ; (4)  $D = 5 \times 10^{-10} \text{ m}^2/\text{s}$ ,  $l = 128 \text{ cm}$ .

distances. Also shown is the theoretical distribution<sup>33</sup> that is expected for this experiment (solid line). Curve 2 shows the signal for the same detector position but for a different diffusion coefficient,  $D = 5 \times 10^{-10} \text{ m}^2/\text{s}$ . The tendency of molecular diffusion to prevent the initial sample plug from being dispersed is obvious. Figure 3 also shows the simulated detector signal for the same value of  $D$  but for detectors located at  $l = 64 \text{ cm}$  and  $l = 128 \text{ cm}$  (no. 3 and no. 4, respectively), together with the theoretical “Taylor curves”.<sup>25</sup> In all four cases, the agreement between simulated and theoretical data is remarkably good. It is concluded that the model works well for describing the analyte flow through a tube under laminar flow conditions. Therefore, it provides an adequate basis for assessing the effects of convection and diffusion on the kinetics observed in continuous-flow experiments. The model could also be useful for describing dispersion phenomena that are encountered in other areas, such as flow-injection analysis.<sup>28</sup>

**Reaction Kinetics Monitored by Continuous-Flow Using a Type I Detector.** Typical examples of age distribution functions for a type I detector are depicted in Figure 4 for  $D = 5 \times 10^{-10} \text{ m}^2/\text{s}$ . The shape of  $P(a)$  depends strongly on the detector position along the tube. The age distribution function in Figure 4A for  $l = 1 \text{ cm}$  is virtually identical to that expected

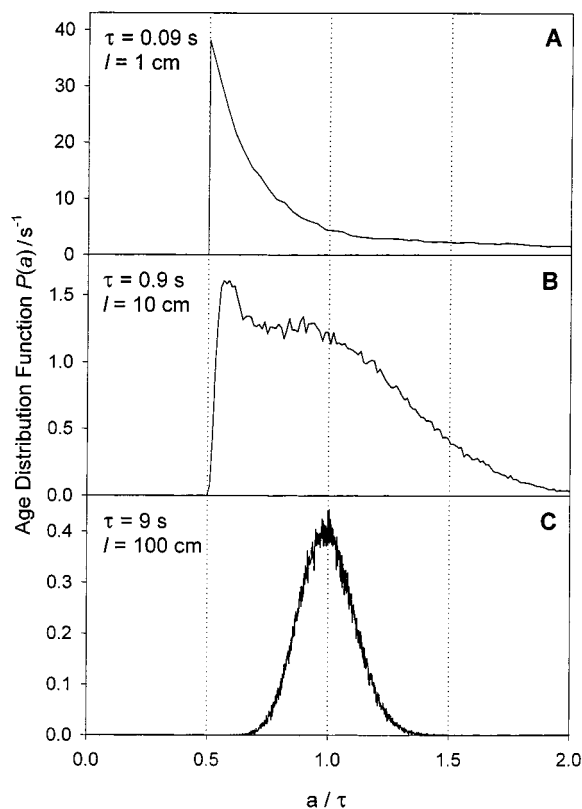


**Figure 4.** Age distribution function as a function of detector position  $l$  for a type I detector and a diffusion coefficient of  $D = 5 \times 10^{-10} \text{ m}^2/\text{s}$ . Tube lengths and the respective values of  $\tau$  are as indicated in the three panels.

in the absence of diffusion (see Figure 1). This is because the residence time of analyte molecules in the tube is too short to allow a notable influence of diffusion. Under these conditions,  $P(a)$  has a maximum at  $a = \tau/2$ . When the distance from the origin to the detector is increased by a factor of 100 (Figure 4C),  $P(a)$  is almost symmetrical and has a maximum around  $a = \tau$ . Again, this effect is due to diffusion which counteracts the dispersion caused by the inhomogeneous velocity profile. Figure 4B represents a situation intermediate between these two extremes;  $P(a)$  still has a maximum close to  $a = \tau/2$  but shows a pronounced shoulder near  $a = \tau$ . All the age distribution functions for type I detectors correspond to an average age of  $\langle a \rangle = \tau$ .

The effects of convection and diffusion on the kinetics observed in continuous-flow experiments are shown in Figure 5. For the sake of simplicity, this comparison is carried out for first-order kinetics where the reactant concentration as a function of time is given by  $C(t) = C_0 e^{-kt}$  with  $C_0 = 1 \text{ mol/L}$ . The concept presented here can easily be applied to more complex cases, and the general phenomena observed will remain the same. The three columns in Figure 5 represent the kinetics for rate constants of  $k = 10 \text{ s}^{-1}$ ,  $k = 1 \text{ s}^{-1}$ , and  $k = 0.1 \text{ s}^{-1}$ , respectively. Results are shown in three rows that correspond to different diffusion coefficients, beginning with  $D = 0$  in the first row. The diffusion coefficient  $D = 1 \times 10^{-10} \text{ m}^2/\text{s}$  used in the second row is a typical value for medium-sized proteins such as lysozyme, myoglobin, or cytochrome *c*. These data describe the situation that is encountered in continuous-flow studies on protein folding.<sup>18,19</sup> The third row uses the value  $D = 5 \times 10^{-10} \text{ m}^2/\text{s}$  representative for molecules about the size of sucrose. Each of the panels in Figure 5 compares a pair of curves. The solid symbols show the kinetics that would be observed in an ideal continuous-flow experiment (homogeneous



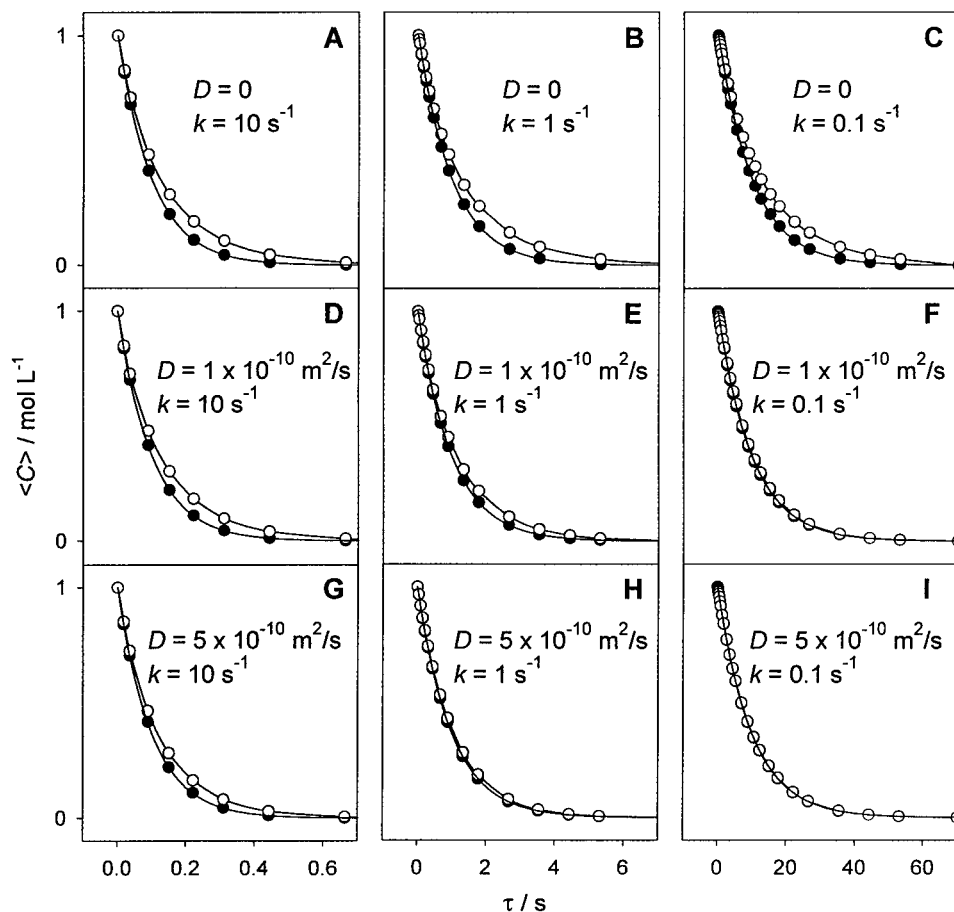


**Figure 5.** Reactant concentration as a function of time  $\tau$ :  $C(\tau) = C_0 e^{-k\tau}$  for  $C_0 = 1 \text{ mol/L}$  and three different values of  $k$  as indicated. Solid symbols correspond to ideal conditions (homogeneous flow), hollow symbols are for laminar flow. These data were simulated for a type I detector. Panels A, B, and C:  $D = 0 \text{ m}^2/\text{s}$ . Panels D, E, and F:  $D = 1 \times 10^{-10} \text{ m}^2/\text{s}$ ; panels G, H, and I:  $D = 5 \times 10^{-10} \text{ m}^2/\text{s}$ . Solid lines are spline curves.

flow), whereas hollow symbols describe the kinetics observed for laminar flow conditions calculated from the corresponding age distribution function by using eq 5. For  $D = 0$  (parts A–C of Figure 5), the deviations between ideal and the realistic curve are most dominant. The maximum deviation occurs at around two half-lives of the reaction when, under homogeneous flow conditions, the average concentration  $\langle C \rangle$  in the tube has decreased to 25%. For laminar flow, it has decreased to about 33% of the initial concentration. Molecular diffusion reduces the extent of these deviations significantly. This effect becomes more pronounced the longer the residence time of the reaction mixture in the tube, as can be seen from parts D–F of Figure 5 for  $D = 1 \times 10^{-10} \text{ m}^2/\text{s}$ . For a short observation window of 0.6 s (Figure 5D), the reduction of the deviation is still small but the discrepancies become successively smaller in the two longer observation windows (Figure 5E,F). For a diffusion coefficient of  $D = 5 \times 10^{-10} \text{ m}^2/\text{s}$  (Figure 5G–I), a notable reduction of these deviations is observed even for the shortest time window. For practical purposes, the differences in Figure 5H are negligible and the two curves shown in Figure 5I are virtually identical.

**Reaction Kinetics Monitored by Continuous-Flow Using a Type II Detector.** Qualitatively, very similar effects are observed when a type II detector is used for monitoring the kinetics. For short residence times in the tube, the age distribution functions for type I and type II detectors are significantly different (see Figure 1). In the limit of long distances between origin and detector and  $D \neq 0$  (e.g.,  $l > 100 \text{ cm}$  for  $D = 1 \times 10^{-10} \text{ m}^2/\text{s}$ ) they become identical (data not shown). For a type II detector, even in the absence of diffusion, the time course of

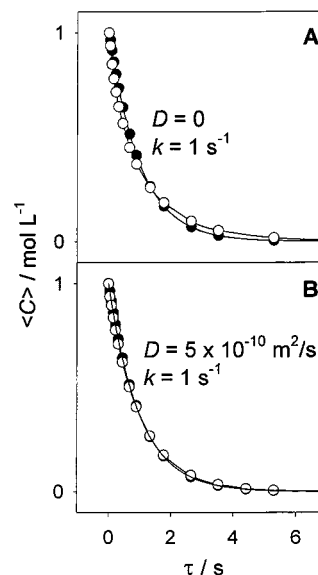


**Figure 6.** Reactant concentration as a function of time as in Figure 5 but for a type II detector. Upper panel,  $D = 0$ ; lower panel,  $D = 5 \times 10^{-10} \text{ m}^2/\text{s}$ .

$\langle C \rangle$  is very similar to the kinetics that would be observed in an ideal continuous-flow experiment (Figure 6A). The largest deviation between both curves occurs roughly after one half-life of the kinetics when  $\langle C \rangle$  has decreased to 50% and 44% of the initial concentration, respectively. On a relative scale, these differences are less than half of those seen for a type I detector under comparable conditions. Again, the deviations become

smaller when the effects of diffusion are taken into account. An example for  $D = 5 \times 10^{-10}$  m<sup>2</sup>/s is shown in Figure 6B.

## Discussion

This theoretical work emerged as the result of a number of recent experimental studies where continuous-flow mass spectrometry (a type I detector) was used to study the kinetics of protein folding,<sup>18,19,23</sup> enzymatic,<sup>20</sup> and bioorganic reactions.<sup>35,36</sup> These studies have demonstrated the enormous potential of mass spectrometry as a new tool for monitoring the kinetics of chemical reactions in solution. However, all these previous studies were carried out in the laminar flow regime, whereas turbulent-flow is widely regarded as an essential requirement for this kind of experiment.<sup>1,2,7,8,14</sup>

In the previous literature, the effects of laminar flow on kinetic continuous-flow measurements in solution have not been examined in great detail.<sup>9</sup> This is in contrast to studies on the kinetics of gas-phase reactions where laminar flow conditions are commonly employed.<sup>21</sup> The processes occurring in gas flow tubes are well understood for a wide range of diffusive regimes.<sup>22</sup> None of these previous studies on gas-phase kinetics take into account specific properties of the carrying medium such as compressibility or mechanisms of heat transfer. Therefore, it should be possible to apply the principles governing these gas-phase processes also to kinetic measurements in solution. If gas flow experiments are carried out at low pressure, radial diffusion is sufficiently fast so that the flow in the reaction tube can be treated as homogeneous. As the pressure is increased, diffusion becomes less effective and the gas in the tube develops a parabolic velocity profile.<sup>21</sup> In a recent study, it has been shown that also under conditions of high pressure and laminar flow the kinetics of gas-phase reactions can be measured with high precision.<sup>22</sup> In that study, a correction method for the observed kinetics is described that is based on an analytical solution of the continuity equation. This method can be used for laminar and turbulent flow conditions. However, in the intermediate regime, where diffusion is neither fast nor slow, the continuity equation cannot be solved analytically and possible asymptotic solutions do not provide an adequate description of the processes in the flow tube. In this regime, the problem has to be treated numerically. The same situation is encountered in the current study that deals with diffusion effects and laminar flow in solution. We could have based this work on a numerical treatment of the continuity equation, but instead a random walk model was chosen that provides a much simpler solution to the problem.

The results of this work allow an assessment of the effects of laminar flow on the reaction kinetics observed in continuous-flow experiments in solution. We shall first discuss the effects of the inhomogeneous velocity profile for conditions where diffusion is negligible, i.e., for short reaction times or for large tube radii ( $R \gg \sqrt{Dt}$ ). These conditions lead to a deviation between the observed and the true concentration–time curves. However, this deviation appears to be surprisingly small, given the odd shape of  $P(a)$  under these conditions (see Figure 1). The effects of the velocity profile on the observed kinetics are less pronounced for type II detectors than for type I detectors because the latter overemphasize contributions from the rapidly flowing molecules near the center of the tube. Where kinetic measurements with high accuracy are required, it will be possible to work out deconvolution procedures that specifically take into account the characteristics of  $P(a)$ . On the basis of the current work, the development of such methods should not be too difficult. These procedures will not be necessary in cases

where it is more important to characterize transient reaction intermediates and to estimate their approximate lifetimes instead of measuring their concentration–time profiles with high accuracy.

The situation is greatly simplified when the dispersion of the age distribution function is reduced by molecular diffusion. For most practical purposes, the differences between measured and true kinetics under these conditions will be negligible, considering the signal-to-noise ratio of the experiment or other limitations such as irregularities in the tube diameter. If diffusion contributes significantly to the age distribution function, it is therefore a good approximation to neglect the effects of laminar flow. Under these conditions, the kinetics can be analyzed as if the flow in the tube was homogeneous. This explains why the continuous-flow kinetics reported by Konermann et al.<sup>18–20</sup> are in good agreement with the results of control experiments using stopped-flow spectroscopy.

The time range that benefits from diffusion effects can be substantially extended by going to smaller tube diameters while leaving the average flow velocity constant. This approach should be especially feasible when modern mass spectrometry based methods are used for signal detection.<sup>37</sup> For the conditions used in this work ( $\bar{v} = 0.113$  and  $R = 37.5 \mu\text{m}$ ), the onset of diffusion effects occurs roughly around  $\tau = 0.5$  s for  $D = 1 \times 10^{-10}$  m<sup>2</sup>/s. From eq 14, it is concluded that the root-mean-square deviation after this time is  $\sqrt{\langle s^2 \rangle} = 2\sqrt{D\tau} = 14 \mu\text{m} \approx R/3$ . Generalizing this result, it follows that the condition for diffusion to have a notable influence on the age distribution function is

$$\tau > \frac{R^2}{36D} \quad (16)$$

As an example, for  $D = 1 \times 10^{-10}$  m<sup>2</sup>/s the onset of diffusion effects in a tube with  $R = 10 \mu\text{m}$  already occurs around  $\tau = 30$  ms. For  $D = 5 \times 10^{-10}$  m<sup>2</sup>/s, this time range would be extended down to around 6 ms.

In view of these findings, turbulent flow no longer appears to be essential for kinetic continuous-flow experiments. Instead, this work clearly indicates the feasibility of kinetic studies in the laminar flow regime. This conclusion has important implications. Maintaining turbulent flow in the observation tube requires the use of very high flow rates and relatively large tube diameters. This leads to considerable sample consumption, even for experiments where high time resolution is not critical. In early continuous-flow studies, as much as 3 L of sample were required for each experiment,<sup>7,8,38</sup> whereas the laminar-flow setup used by Konermann et al.<sup>18–20,23</sup> operates on a milliliter scale. Miniaturized continuous-flow devices achieve a time resolution on the order of tens of milliseconds or better, can be easily assembled, and require no high-pressure pumps. When these devices are used in conjunction with electrospray ionization mass spectrometry, they can give valuable kinetic information that is often not accessible by other methods. It is hoped that this study will contribute to a more widespread use of this elegant, simple, and inexpensive method for monitoring the kinetics of chemical reactions.

**Acknowledgment.** The author thanks Professor Derek G. Leaist for helpful discussions and critical reading of the manuscript. Financial support for this work was provided by The Natural Sciences and Engineering Research Council of Canada and The University of Western Ontario.

## References and Notes

- (1) Fersht, A. *Structure and Mechanism in Protein Science*; W. H. Freeman & Co.: New York, 1999.

- (2) Johnson, K. A. *Methods Enzymol.* **1995**, 249, 38–61.
- (3) Crouch, S. R.; Holler, F. J.; Notz, P. K.; Beckwith, P. M. *Appl. Spectrosc. Rev.* **1977**, 13, 165–259.
- (4) Gibson, Q. H. *Methods Enzymol.* **1969**, XVI, 187–228.
- (5) Roder, H.; Elöve, G. A.; Englander, S. W. *Nature* **1988**, 335, 700–704.
- (6) Miranker, A.; Robinson, C. V.; Radford, S. E.; Aplin, R.; Dobson, C. M. *Science* **1993**, 262, 896–900.
- (7) Hartridge, H.; Roughton, F. J. W. *Proc. R. Soc. (London)* **1923**, A104, 376–394.
- (8) Gutfreund, H. *Methods Enzymol.* **1969**, XVI, 229–249.
- (9) Roughton, F. J. W.; Millikan, G. A. *Proc. R. Soc. (London)* **1936**, A155, 258–268.
- (10) Roughton, F. J. W. *Proc. R. Soc. (London)* **1936**, A155, 269–276.
- (11) Millikan, G. A. *Proc. R. Soc. (London)* **1936**, A155, 277–292.
- (12) Shastri, M. C. R.; Luck, S. D.; Roder, H. *Biophys. J.* **1998**, 74, 2714–2721.
- (13) Shastri, M. C. R.; Roder, H. *Nat. Struct. Biol.* **1998**, 5, 385–392.
- (14) Owens, G. D.; Margerum, D. W. *Anal. Chem.* **1980**, 52, 91A–106A.
- (15) Jacobs, S. A.; Nemeth, M. T.; Kramer, G. W.; Ridley, T. Y.; Margerum, D. W. *Anal. Chem.* **1984**, 56, 1058–1065.
- (16) Wiskind, H. K. On the Application of Fluid Dynamics to the Development of Rapid Mixing Techniques. Proceedings of the First International Colloquium on Rapid Mixing and Sampling Techniques Applicable to the study of Biochemical Reactions, Philadelphia, 1964.
- (17) Probstein, R. F. *Physicochemical Hydrodynamics*, 2nd ed.; John Wiley & Sons: New York, 1994.
- (18) Koneremann, L.; Rosell, F. I.; Mauk, A. G.; Douglas, D. J. *Biochemistry* **1997**, 36, 6448–6454.
- (19) Koneremann, L.; Collings, B. A.; Douglas, D. J. *Biochemistry* **1997**, 36, 5554–5559.
- (20) Zechel, D. L.; Koneremann, L.; Withers, S. G.; Douglas, D. J. *Biochemistry* **1998**, 37, 7664–7669.
- (21) Howard, C. J. *J. Phys. Chem.* **1979**, 83, 3–9.
- (22) Donahue, N. M.; Clarke, J. S.; Demerjian, K. L.; Anderson, J. G. *J. Phys. Chem.* **1996**, 100, 5821–5838.
- (23) Chen, Y.-L.; Campbell, J. M.; Collings, B. A.; Koneremann, L.; Douglas, D. J. *Rapid Commun. Mass Spectrom.* **1998**, 12, 1003–1010.
- (24) Koneremann, L. *Sci. Prog.* **1998**, 81, 123–140.
- (25) Taylor, G. *Proc. R. Soc. (London)* **1953**, A219, 186–203.
- (26) Robinson, B. H. Rapid Flow Methods. In *Investigation of Rates and Mechanisms of Reactions, Part II*; Bernasconi, C. F., Ed.; John Wiley & Sons: New York, 1986; Vol. VI, pp 9–25.
- (27) Laidler, K. J.; Meiser, J. H. *Physical Chemistry*, 3rd ed.; Houghton Mifflin Company: Boston, New York, 1999.
- (28) Ruzicka, J.; Hansen, E. H. *Flow Injection Analysis*, 2nd ed.; John Wiley & Sons: New York, 1988; Vol. 62.
- (29) Vanderslice, J. T.; Stewart, K. K.; Rosenfeld, A. G.; Higgs, D. J. *Talanta* **1981**, 28, 11–18.
- (30) Bate, H.; Rowlands, S.; Sirs, J. A.; Thomas, H. W. *J. Phys. D* **1969**, 2, 1447–1456.
- (31) Bate, H.; Rowlands, S.; Sirs, J. A. *J. Appl. Physiol.* **1973**, 34, 866–872.
- (32) van Akker, E. B.; Bos, M.; van der Linden, W. E. *Anal. Chim. Acta* **1999**, 378, 111–117.
- (33) Gill, W. N.; Sankarasubramanian, R. *Proc. R. Soc. (London)* **1970**, A316, 341–350.
- (34) Aris, R. *Proc. R. Soc. (London)* **1956**, A235, 67–77.
- (35) Sam, J. W.; Tang, X. J.; Peisach, J. *J. Am. Chem. Soc.* **1994**, 116, 5250–5256.
- (36) Sam, J. W.; Tang, X. J.; Magliozzo, R. S.; Peisach, J. *J. Am. Chem. Soc.* **1995**, 117, 1012–1018.
- (37) Wilm, M.; Mann, M. *Anal. Chem.* **1996**, 68, 1–8.
- (38) Hartridge, H.; Roughton, F. J. W. *Proc. R. Soc. (London)* **1923**, A104, 395–430.